Performance and Complexity of Turbo Equalizers for optical coherent Gbit/s Transmission with optimal and suboptimal Detection Strategies

Klaus Oestreich, Joachim Speidel

Universität Stuttgart, Institut für Nachrichtenübertragung, 70569 Stuttgart
E-Mail: klaus.oestreich@inue.uni-stuttgart.de

Abstract

In this paper, we investigate two different turbo equalizers with distinct detection strategies for coherent optical communication with QPSK modulated signals. The first receiver comprises a BCJR detector and a soft-in soft-out LDPC decoder. In the second receiver, the BCJR unit is replaced by a linear MMSE filter. Offering enough turbo iterations for the receiver with MMSE detection, the performance is almost the same as for the receiver with the optimal BCJR detection. As the computational complexity of the MMSE detection is considerable lower as for the BCJR detection, the turbo equalizer with MMSE detection offers a good compromise between complexity and performance.

1 Introduction

Turbo equalization as an iterative approach of detection and decoding provides tremendous performance gains for communication systems suffering from intersymbol interference (ISI) and noise. The principle of turbo equalization was introduced by C. Douillard et al. in [1]. This scheme applies the so called "turbo-principle" presented by Berrou et al. [2] two years before for iterative decoding. Due to the outstanding performance of this approach, turbo equalization has been rapidly adapted to mobile communication systems [3] and has also gained interest in optical communications.

For an intensity modulated optical communication system turbo equalization has been discussed in [4] and [5]. In [6] we presented a turbo equalizer for quadrature phase shift keying (QPSK) optical coherent Gbit/s transmission. In this investigations a Bahl, Cocke, Jelinek and Raviv (BCJR) detector [7] is used for soft-in soft-out (SISO) detection and a low-density parity-check (LDPC) SISO decoder for forward error correction (FEC). It has been proven, that this turbo equalizer owns a considerable performance.

The BCJR detector operates with a maximum a posteriori (MAP) symbol-by-symbol (sbs) method. It is the most powerful detection algorithm which can be used for the turbo equalizer. However, the computational complexity increase exponentially with the channel length. Thus, we investigate in this paper a linear detector as a suboptimal detection strategy. The filter coefficients are updated according to the Minimum Mean Squared Error (MMSE) criteria with the advantage that the computational complexity is much smaller compared to the MAP-solution.

For FEC LDPC codes with an overhead between 6.7% to 14.3% are used. They do not extend the signal bandwidth aggressively and offer a good compromise between high error correction performance and complexity. For SISO decoding, the so called sum-product-algorithm (SPA) decoder [8] is used, which is an iterative sbs-MAP algorithm with high performance.

This paper is organized as follows. In section 2 the model of the coherent optical system with the turbo equalization is introduced. The algorithm of the linear MMSE detector using *a priori* information is presented in section 3. In section 4 a comparison of the computational complexity of the BCJR and MMSE detectors are given. Based on simulation results the performance of the turbo equalizer is evaluated in section 4, and section 5 concludes the paper.

2 System Model

Our investigations are based on the coherent optical system of **Fig. 1**. The basic elements are the transmitter (TX), the standard single mode fiber (SSMF) and the optically preamplified receiver (RX) comprising the turbo equalizer. As indicated in the block diagram, the turbo equalizer consists of the SISO detector and the SISO decoder. As a detector, the BCJR and an MMSE detector are considered alternatively. For decoding we use the iterative sum product algorithm (SPA) decoder as described in [6]. The turbo equalizer contains a feedback loop from the decoder to the detector. By passing extrinsic information between the detector and the decoder the performance can be improved in each turbo iteration. As indicated in **Fig. 1** no interleaver and deinterleaver are used in the turbo loop as they are not required for the applied LDPC codes.

The information bits b_k to be transmitted have the bit rate $R_b = 40\,\mathrm{Gb/s}$. For FEC at the receiver, the LDPC encoder adds redundancy to the information bits. The binary symbols $\mathbf{c}_n = [c_{n,1}\ c_{n,2}]$ are fed into a time domain raised cosine impulse shaper with roll-off factor 0.35 for non-return-to-zero (NRZ) impulse generation. Finally an optical QPSK modulator (QM) consisting

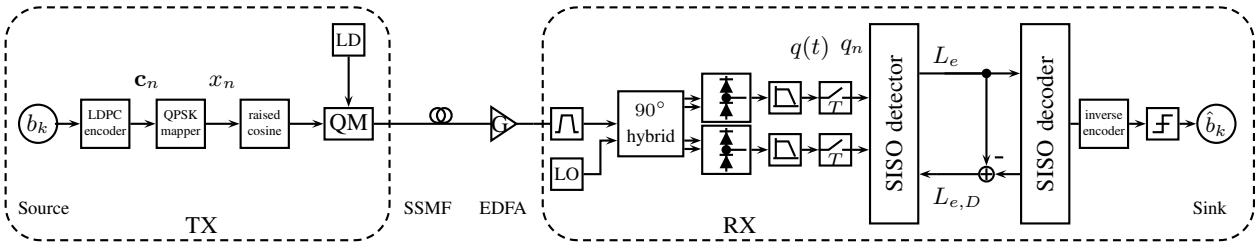

Fig. 1: Transmitter, fiber and receiver of coherent system with turbo equalization.

of two Mach-Zehnder modulators (MZM) provides the optical tx-signal.

The symbol rate on the fiber is

$$R_s = \frac{R_b}{M' \cdot R_c}, \tag{1}$$

with M' = 2 as a 4-ary modulation scheme is used. R_c is the code rate of the LDPC code. Along the fiber the optical signal is affected by chromatic dispersion (CD) and attenuation. An erbium doped fiber amplifier (EDFA) at the receiver side with amplification factor G completely compensates the loss of the fiber. This amplifier is the major source of noise in the transmission system. The amplified spontaneous emission (ASE) noise is modeled by a two dimensional complex additive white Gaussian noise (AWGN) process with a spectral noise power density $N_{0,pol,real}$ per spatial and complex dimension. The total spectral noise power density is $N_0 = 4N_{0,pol,real}$. The optical signal-to-noise ratio (OSNR) in dB is defined as

$$\text{OSNR} = 10\log\left(\frac{\overline{P}_{opt}}{N_0 B_{opt}}\right). \tag{2}$$

$B_{opt} = 12.5\,\text{GHz}$ is the optical measurement bandwidth and $\overline{P}_{opt}$ the mean optical symbol power. For a bit rate of $R_b = 40\,\text{Gb/s}$ the relationship between the signal to noise ratio per information bit and the OSNR is

$$\begin{aligned}\frac{E_b}{N_0} &= \text{OSNR} - 10\log R_b + 10\log B_{opt} \\ &\approx \text{OSNR} - 5.05\,\text{dB}.\end{aligned} \tag{3}$$

In a first step at the receiver a Gaussian optical bandpass filter of 2nd order with a 3dB-bandwidth $\Delta B_{3dB} = 2R_b$ reduces the impact of the noise and serves as a WDM demultiplexer. Then a 90° hybrid and two balanced photo diodes serve as an optical I-Q-demodulator, delivering the electrical inphase (I) and quadrature (Q) component of the demodulated QPSK signal. As the receiver electronics exhibit a lowpass characteristic, a 3rd order Bessel filter with 3dB-cut-off-frequency $f_{3dB} = 0.5R_b$ is inserted in the system to model this aspect. The electrical signal $q(t)$ is sampled at time instants $t = nT_s + t_0$. $T_s = 1/R_s$ is the interval of the QPSK symbols, and $n \in \mathbb{Z}$.

Finally the samples q_n provides the input for the turbo equalizer. The estimates $\hat{b}_k$ of the transmitted bit sequence b_k are available after inverse encoding and hard decision of the decoded bitstream.

In the following the algorithms for BCJR and particularly MMSE detection are described in more detail.

3 Equalization

The turbo equalizer has to be designed to utilize *a priori* information for the calculation of the extrinsic information. In the following we present the optimal BCJR detector and a linear MMSE detector as a suboptimal but less complex solution.

3.1 BCJR algorithm

The BCJR algorithm is a trellis based forward-backward scheme, developed by L. Bahl, J. Cocke, F. Jelinek and J. Raviv [7]. As an MAP detection, symbol-by-symbol approach it provides the optimal detection strategy with respect to minimizing the bit error rate (BER).

The algorithm can be implemented in the probability domain or in the log domain as described e.g. in [9]. Implementation in the log domain is less complex, as it is based on additions rather than on multiplications. Therefore we use the log domain algorithm for our investigations. The algorithm is not explained in all aspects here, as a detailed description can be found in [6].

As we will see in section 4, the computational complexity of the BCJR algorithm increases exponentially with the channel length. Thus, we examine a less complex linear MMSE detector in detail in the following.

3.2 Linear MMSE detector

The MMSE detector is based on a linear filter with coefficients which are determined to minimize the cost function $J = \mathrm{E}\left(|x_n - \hat{x}_n|^2\right)$, where x_n is the transmit symbol and $\hat{x}_n$ is the linear estimate of x_n as output of the MMSE detector.

To solve this minimization problem, the channel coefficients h_k, $k = 0, 1, \ldots, M-1$ and the noise variance σ_w^2 have to be known at the receiver. Both are estimated based on a pilot signal.

Based on the channel coefficients we define a channel convolution matrix

$$\mathbf{H} \doteq \begin{bmatrix} h_{M-1} & h_{M-2} & \cdots & h_0 & \cdots & & 0 \\ 0 & h_{M-1} & h_{M-2} & \cdots & h_0 & \cdots & 0 \\ & & & \ddots & & & \\ 0 & \cdots & 0 & h_{M-1} & h_{M-2} & \cdots & h_0 \end{bmatrix}$$

Let $N = N_1 + N_2 + 1$ be the overall finite impulse response (FIR) filter length of the detector with a non-causal part of length N_1 and a causal part of length N_2. We define the vector

$$\mathbf{s} \doteq \mathbf{H}\begin{bmatrix}\mathbf{0}_{1\times(N_2+M-1)} & 1 & \mathbf{0}_{1\times N_1}\end{bmatrix}^T. \tag{4}$$

The optimal filter coefficient vector of the MMSE detector are then given by

$$\mathbf{f} = \left(\sigma_w^2 \mathbf{I}_N + \mathbf{H}\mathbf{H}^{\mathrm{H}}\right)^{-1} \mathbf{s}. \tag{5}$$

$\mathbf{I}_N$ is the $N \times N$ identity matrix and $()^{\mathrm{H}}$ denotes the Hermitian operator. Filtering the sampled receive signal

$$\mathbf{q}_n \doteqdot \begin{bmatrix} q_{n-N_2} & q_{n-N_2+1} & \cdots & q_{n+N_1} \end{bmatrix}^T$$

by the MMSE detector provides estimates of the symbols x_n:

$$\hat{x}_n = \mathbf{f}^{\mathrm{H}} \mathbf{q}_n \tag{6}$$

For the turbo equalizer the extrinsic log-likelihood ratio (LLR) values are required, rather than the estimated symbols. According to [10], the MMSE detector can be extended to cope with this issue. For QPSK mapping, the two LLR values per symbol are computed as follows.

$$\begin{aligned} L_e\left(c_{n,1}\right) &= \frac{\sqrt{8}}{1 - \mathbf{s}^{\mathrm{H}}\mathbf{f}} \operatorname{Re}\left(\mathbf{f}^{\mathrm{H}}\mathbf{q}_n\right) \\ L_e\left(c_{n,2}\right) &= \frac{\sqrt{8}}{1 - \mathbf{s}^{\mathrm{H}}\mathbf{f}} \operatorname{Im}\left(\mathbf{f}^{\mathrm{H}}\mathbf{q}_n\right) \end{aligned} \tag{7}$$

This method does not take *a priori* information into account. As a consequence the filter coefficients $\mathbf{f}$ are independent of n. Thus, they need to be computed only once, as far as the channel coefficients do not change. In the following we will explain, how we can extend the algorithm to include *a priori* information. This is necessary, if several turbo iterations shall be performed.

3.3 Linear MMSE detector considering *a priori* knowledge

How to include the *a priori* knowledge in the linear MMSE detector is explained in [10]. Both extrinsic LLR values $L_{e,D}\left(c_{n,i}\right)$ of one symbol from the decoder are considered in the computation of the mean and variance of the transmitted QPSK symbols:

$$\overline{x}_n = \frac{1}{\sqrt{2}} \left(\tanh\left(\frac{L_{e,D}\left(c_{n,1}\right)}{2}\right) + j \tanh\left(\frac{L_{e,D}\left(c_{n,2}\right)}{2}\right)\right) \tag{8}$$

$$v_n = 1 - \left|\overline{x}_n\right|^2 \tag{9}$$

With v_n we define the matrix

$$\begin{aligned} \mathbf{V}_n &= \operatorname{Cov}\left(\mathbf{x}_n, \mathbf{x}_n\right) \\ &= \operatorname{diag}\begin{bmatrix} v_{n-M-N_2+1} & \cdots & v_{n+N1} \end{bmatrix} \end{aligned} \tag{10}$$

This matrix is used to compute the filter coefficients

$$\mathbf{f}_n = \left(\sigma_w^2 \mathbf{I}_N + \mathbf{H}\mathbf{V}_n\mathbf{H}^{\mathrm{H}}\right)^{-1} \mathbf{s} \tag{11}$$

including the *a priori* information on x_n. As $\mathbf{f}_n$ depends on time (time-varying coefficients), the filter coefficients have to be calculated for each n. Finally,

$$\begin{aligned} L_e\left(c_{n,1}\right) &= \frac{\sqrt{8}}{1 - v_n \mathbf{s}^{\mathrm{H}}\mathbf{f}_n} \operatorname{Re}\left(\mathbf{f}_n^{\mathrm{H}}\left(\mathbf{q}_n - \mathrm{E}\left(\mathbf{q}_n\right) + \overline{x}_n\mathbf{s}\right)\right) \\ L_e\left(c_{n,2}\right) &= \frac{\sqrt{8}}{1 - v_n \mathbf{s}^{\mathrm{H}}\mathbf{f}_n} \operatorname{Im}\left(\mathbf{f}_n^{\mathrm{H}}\left(\mathbf{q}_n - \mathrm{E}\left(\mathbf{q}_n\right) + \overline{x}_n\mathbf{s}\right)\right) \end{aligned} \tag{12}$$

holds for the extrinsic output of the detector.

4 Complexity of the detectors

In order to compare the BCJR and MMSE detector we first give a rough estimation of their computational complexity, i.e. the number of arithmetic operations. Memories to buffer the signals required for hardware implementation are not considered here. We further neglect the estimation of the channel for the MMSE detector and of the probability density functions (PDFs) for the BCJR, respectively.

To reduce complexity, often only $\nu < M$ channel coefficients h_k are taken into account for detection. In the best case, $\nu = M$ holds. The BCJR algorithm is based on the trellis diagram. The complexity of the algorithm grows with the number of states and branches in the trellis. The number of states per time instant n for QPSK-modulated signals is 4^ν and the number of branches or state transitions is $4^{\nu+1}$. For $\nu = 4$ the trellis has 256 states and 1024 state transitions per time instant n, for $\nu = 6$ these numbers are 4096 and 16384, respectively.

Due to this exponential increase of branches and states, channels with a long impulse response as well as a large QAM constellation size lead to a high computational complexity. The number of complex additions to compute the metrics as well as the LLR values for one instant of time n is given in **Table 1**. The total number of complex additions in case no *a priori* information is considered results in

$$2\left(4^{\nu+2} + 4^{\nu+1} + 6 \cdot 4^\nu + 1\right) \tag{13}$$

per time instant. Taking *a priori* information into account we get

$$3\left(4^{\nu+2} + 4^{\nu+1}\right) + 2. \tag{14}$$

In a turbo equalizer for each data sequence the BCJR algorithm is executed several times. Thus, the computational complexity is even higher. However, in [5] and [6] it was shown, that for LDPC coded turbo equalization one detection procedure is enough. The gain of a turbo equalizer performing ten decoder iterations and nine iterations over the turbo equalizer compared to one detection followed by 24 iterations of the decoder is only some tenths of dB. Thus, the complexity can be reduced without a significant performance loss, if the feedback loop between the decoder and detector is omitted.

Based on this results we evaluate the performance of a receiver, where a linear MMSE detector is concatenated with an LDPC decoder. Omitting the feedback loop also significantly reduces the complexity of the MMSE detector. This is due to the fact, that the filter coefficient vector $\mathbf{f}$ needs to be calculated only ones as it does not dependent on time anymore. As a consequence, the inverse of the $N \times N$ matrix $\mathbf{H}\mathbf{H}^{\mathrm{H}}$ has to be calculated only ones.

Using *a priori* information, the inverse matrix in (11) has to be computed for each time instant n. The complexity of a matrix inversion is of order $\mathcal{O}\left(N^3\right)$ which mostly determines the complexity of the MMSE detector described in section 3.3. However, in [10] a recursive

	comment	complex additions
$\tilde{\gamma}_n$	In case no *a priori* information is used (no Turbo iteration) no additions are required. Otherwise the probability density function (PDF) value and two (in case of QPSK) LLR values have to be added. There are $4^{\nu+1}$ branches in total per n.	0 / $2 \cdot 4^{\nu+1}$
$\tilde{\alpha}_n$	For each of the $4^{\nu+1}$ branches a forward metric has to be calculated, requiring one addition per branch. Then for each of the 4^{ν} states, one of 4 metrics have to be selected. We approximate the computational complexity of the max-operation with 4 input values by 3 times the complexity of one addition. Per selected metric, 3 additions of a correction term have to be performed. The correction terms are stored in a look-up table.	$4^{\nu+1} + 6 \cdot 4^{\nu}$
$\tilde{\beta}_{n-1}$	Same complexity as for $\tilde{\alpha}_n$.	$4^{\nu+1} + 6 \cdot 4^{\nu}$
$L_e\left(c_{n,i}\right)$	For each of the $4^{\nu+1}$ branches $\tilde{\alpha}_{n-1}$, $\tilde{\beta}_n$ and $\tilde{\gamma}_n$ have to be summed up $(2 \cdot 4^{\nu+1})$. The selection of the maximum values is estimated with a complexity of $4^{\nu+1}$. The summation of the correction terms requires $4^{\nu+1}$ further additions. Finally, the difference of the maximum of two sets of state transitions have to be calculated (one further addition). For QPSK two LLR values have to be calculated per n.	$2\left(4^{\nu+2}+1\right)$

Table 1: Computational complexity of the BCJR algorithm.

algorithm to compute $\mathbf{f}_n$ is presented with a complexity of only $\mathcal{O}\left(N^2\right)$.

In [11] the number of real multiplications for this recursive algorithm is given as

$$16N^2 + 4\nu^2 + 10\nu - 4N - 4 \tag{15}$$

and the number of real additions as

$$8N^2 + 2\nu^2 - 10N + 2\nu + 4. \tag{16}$$

(15) and (16) from [11] do not take into account the following calculations: the statistics for $\overline{x}_n$ and v_n for all n, $L_e\left(c_{n,i}\right)$, the the estimation of the channel coefficients h_k and the noise variance σ_w^2. Moreover, for each branch of the BCJR-algorithm one PDF has to be estimated. As there are $4^{\nu+1}$ branches, this computational complexity is higher than that for the channel estimation and is not considered in (13) and (14). As a consequence, a longer training sequence is necessary to estimate the PDFs than to estimate the channel coefficients h_k.

For comparison of the computational complexity of the BCJR and MMSE detectors, the amount of real additions and multiplications are given in **Table 2**. As can be

	BCJR real additions		MMSE	
ν	no *a priori*	*a priori*	mult.	add.
2	1668	1924	1924	874
4	26 628	30 724	2752	1266
5			3226	1492
6	425 988	491 524	3740	1738
7			4294	2004
9			5522	2596

Table 2: Number of real additions and multiplications for the BCJR and MMSE algorithm per n and per iteration.

seen, the difference is significant, especially if $\nu = 6$ for the BCJR is necessary. The suboptimal MMSE solution is much less complex even if more turbo iterations are performed.

5 Performance of the turbo equalizers

We use regular codes based on Euclidian or projective geometries for the investigation of the performance of the turbo equalizer. **Table 3** presents three codes which have proven to own an outstanding BER performance [6] for a turbo equalizer based on BCJR detection. Their code overhead is between 5 and 15%. The computer simulations presented in this section for the system with MMSE detection are based on these codes.

Fig. 2 shows the BER vs. OSNR and compares the turbo equalizer with MMSE detection for all listed LDPC codes and for the turbo equalizer with BCJR detection for LDPC code 2. These simulation results are for a back-to-back arrangement, i.e. a fiber length of $l = 0\,\mathrm{km}$ or a residual chromatic dispersion of $R_D = 0$.

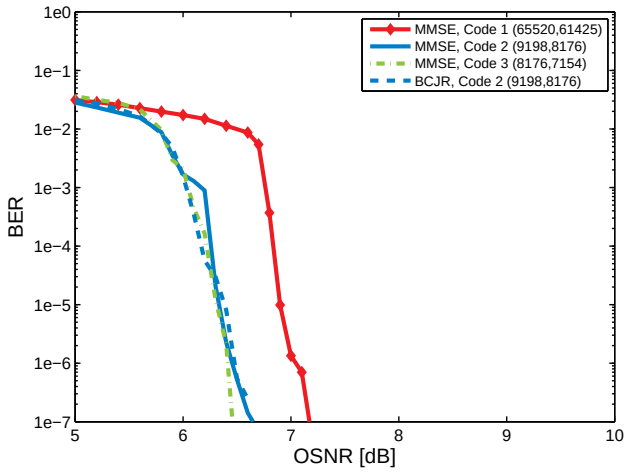

Fig. 2: BER vs. OSNR of the RX with turbo equalization for different detectors and LDPC codes, $R_D = 0$, $R_b = 40\,\mathrm{Gbit/s}$.

For these results, the feedback loop of the turbo equalizer is dropped. Thus, equalization is performed only onces without considering *a priori* information. The SPA decoder performs 24 iteration. In the following this scenario is indicated by $\iota_t = 0/\iota_d = 24$, where ι_t denotes the number of turbo iterations (loop detector-decoder) and ι_d denotes the number of iterations of the LDPC decoder (decoder loop). $\iota_t = 0$ means, the turbo loop is not active and there is only one pass. The same hold for $\iota_d = 0$. Consequently, 1/24 means, that the turbo loop is active and the detection algorithm performs twice while the LDPC decoder operates with 24 iterations for each turbo iteration. So, in this case, the LDPC decoder provides extrinsic information for the detector.

The performance difference of both detection schemes

	N	K	$N-K$	R_c	O_c	c	ρ	γ	J
Code 1	65520	61425	4095	0.938	6.7%	1	64	4	4095
Code 2	9198	8176	1022	0.889	12.5%	9	27	3	1022
Code 3	8176	7154	1022	0.875	14.3%	8	32	4	1022

Table 3: Selected LDPC codes. N: codeword length, K: information word length, R_c: code rate $R_c = K/N$, O_c: code overhead $O_c = 1 - R_c^{-1}$, c: number of square matrices that compose the code, ρ: row weight, γ: column weight, J: number of rows in the parity check matrix.

is small, as there is no ISI for $R_D = 0$. We also see, that the performance of code 1 is worse compared to code 2 and 3. The performance of the turbo equalizer with code 3 is slightly better than for code 2. This is confirmed by **Fig. 3**, a plot of the required OSNR at a BER of 10^{-7} as a function of the residual chromatic dispersion R_D. Especially for moderate R_D the difference between code 2 and 3 is marginal. As the overhead and the complexity of code 2 are smaller than for code 3, we use code 2 for our further investigations.

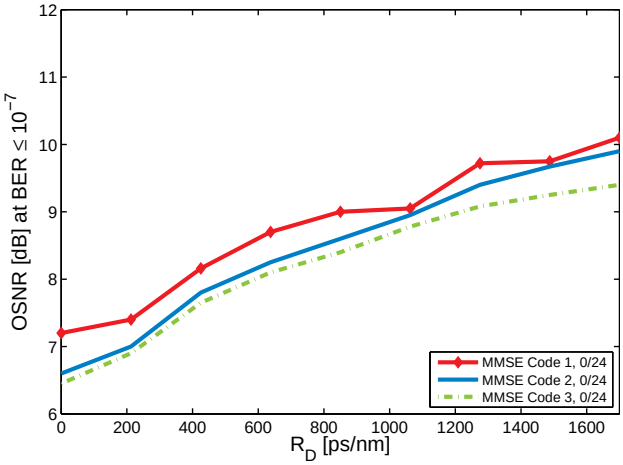

Fig. 3: Required OSNR versus residual chromatic dispersion R_D for a MMSE detector and different LDPC codes operating at BER of 10^{-7} and at R_b = 40 Gbit/s.

In **Fig. 4** we present the required OSNR to achieve a BER $\leq 10^{-7}$ for a turbo equalizer with BCJR and MMSE detector. Our simulations have shown that a receiver with $\iota_t = 0$, large ι_d and BCJR detection exhibits almost the same performance as receivers $\iota_t > 1$ (see later in **Fig. 5**). That means, that the turbo iterations do not lead to a significant gain for a receiver with BCJR detection. Thus, only the results for 0/24 of the BCJR are depicted in **Fig. 4**. For the turbo equalizer with MMSE detection several scenarios ι_t/ι_d are plotted.

The number of channel coefficients considered for the simulations are indicated in **Table 4**. As the complexity of the BCJR detector grows exponentially with ν, we used a smaller ν than for the MMSE detector, although the comparison lacks some fairness. This is the reason, why the graph of the BCJR detector does not grow smoothly but exhibits a kink.

From the results of **Fig. 4** we can conclude, that the performance is almost the same for all schemes in the range of small residual dispersion R_D. For large R_D a

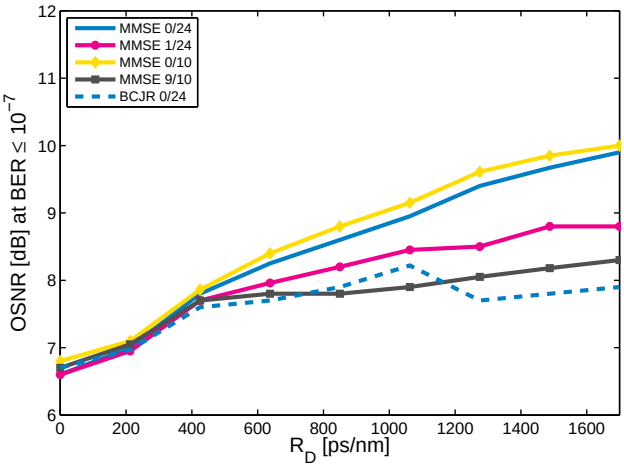

Fig. 4: Required OSNR versus residual chromatic dispersion R_D for different detectors and LDPC code 2 operating at BER of 10^{-7} and at R_b = 40 Gbit/s.

large gain can be achieved by the turbo equalizer with MMSE detection, if $\iota_t = 1$ or even 9 turbo iterations are running. This gain is depicted in **Fig. 5**. There we see,

R_D [ps/nm]	ν (BCJR)	ν (MMSE)
0	2	1
212.5	2	3
425	4	5
637.5	4	5
850	4	7
1062.5	4	7
1275	6	9
1487.5	6	9
1700	6	9

Table 4: Number of channel coefficients considered in the simulations for BCJR and MMSE detection in dependence of R_D. Further we used $N_2 = \nu$ and $N_1 = 9$ for the MMSE detector.

that if the information from the decoder is fed back to the MMSE detector at least ones ($\iota_t = 1$), the gain for large R_D is already more than 1 dB. If we spend $\iota_t = 9$ turbo iterations, the number of decoder iterations ι_d can be decreased. The gain with 9 turbo iterations and ten decoder iterations is larger than 1.5 dB in the region of high R_D.

Comparing the performance of the receiver with BCJR and MMSE detection, we can conclude, that the difference is only marginal for small residual chromatic dispersion. For complexity reasons, the receiver with MMSE detection without iterations over the turbo equalizer is the preferred choice. For larger R_D the difference can be

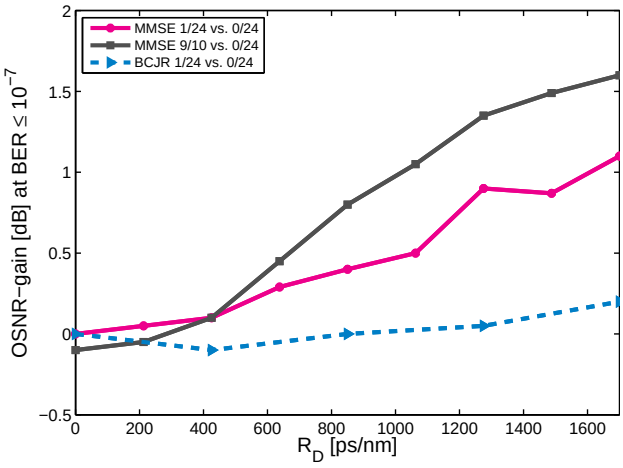

Fig. 5: OSNR gain of the turbo equalizer with MMSE detection with $\iota_t = 1$ and $\iota_t = 9$ turbo iteration in comparison to no turbo iteration and of the turbo equalizer with BCJR detection $\iota_t = 1$ turbo iteration in comparison to no turbo iteration, $R_b = 40\,\mathrm{Gbit/s}$.

made small as well, if we spend more turbo iterations for the receiver with MMSE detection.

6 Conclusion

We have investigated optimal and suboptimal turbo equalizers for optical coherent transmission at a bit rate of $40\,\mathrm{Gbit/s}$. The first receiver under study consists of a BCJR detector and a SISO LDPC decoder. In the second receiver, the BCJR algorithm is replaced by a linear filter with coefficients updated according to the MMSE criteria.

It is shown, how to provide the MMSE detector with *a priori* knowledge from the LDPC decoder and how to calculate extrinsic LLR values. This extension is required for the turbo equalizer, where the extrinsic LLR values of the decoder are used as *a priori* information at the detector.

The simulation of the performance of both receivers are based on three different finite geometry LDPC codes with overhead in the range of 6.7% and 14.3%. In previous investigations these codes have proven to own excellent BER performance while keeping the complexity of the decoder low. For the simulations a channel with different residual chromatic dispersions are considered.

We found out, that both receivers have almost the same performance in the region of low residual chromatic dispersion R_D. For higher chromatic dispersions the turbo equalizer with MMSE detection benefits from the feedback of the extrinsic LLR values of the decoder. In case nine turbo iterations are performed there is a gain of more than $1.5\,\mathrm{dB}$ at $R_D = 1600\,\mathrm{ps/nm}$ compared to a receiver with no turbo iteration.

The computational complexity of the BCJR detector grows exponentially with the channel length. The complexity of the MMSE detector with N filter coefficients is only of order $\mathcal{O}\left(N^2\right)$. The BER performance of a turbo receiver with MMSE detector, nine turbo iterations and ten LDPC decoder iterations is almost the same as for the receiver with the optimal but much more complex BCJR detection. Thus, the turbo equalizer with MMSE detection offers a good compromise between complexity and performance.

Acknowledgement

This work was carried out in the framework of the project "Coding and equalization for coherent optical communication systems" and funded by Deutsche Forschungsgemeinschaft (DFG) which is gratefully acknowledged.

References

[1] C. Douillard, M. Jézéquel, C. Berrou, P. Didier, and A. Glavieux, "Iterative correction of intersymbol interference: Turbo-equalization," *European Trans. Telecommunications*, vol. 6, pp. 259 – 511, Sep./Oct. 1995.

[2] C. Berrou, A. Glavieux, and P. Thitimajshima, "Near shannon limit error-correcting coding and decoding: Turbo-codes. (1)," in *IEEE International Conference on Communications, 1993. ICC '93 Geneva. Technical Program, Conference Record.*, vol. 2, May 1993, pp. 1064 –1070.

[3] G. Bauch, H. Khorram, and J. Hagenauer, "Iterative equalization and decoding in mobile communications systems," in *Second European Personal Mobile Communications Conference (2. EPMCC '97*, 1997, pp. 307–312.

[4] M. Jäger, T. Rankl, J. Speidel, H. Bülow, and F. Buchali, "Performance of turbo equalizers for optical PMD channels," *J. Lightw. Technol.*, vol. 24, no. 3, pp. 1226–1236, Mar. 2006.

[5] T. Rankl, C. Kurz, and J. Speidel, "Performance bounds of optical receivers with electronic detection and decoding," *J. Lightw. Technol.*, vol. 27, no. 16, pp. 3567–3579, Aug. 2009.

[6] K. Oestreich and J. Speidel, "Investigation of near optimum iterative equalizers and decoders for optical coherent Gbit/s transmission." *ITG Symposium on Photonic Networks, Leipzig*, May 2012.

[7] L. Bahl, J. Cocke, F. Jelinek, and J. Raviv, "Optimal decoding of linear codes for minimizing symbol error rate," *IEEE Trans. Inf. Theory*, vol. 20, pp. 284–287, Mar 1974.

[8] S. Lin, J. Daniel, and J. Costello, *Error control coding*. Prentice Hall, New York, 2005.

[9] W. E. Ryan, *Wiley Encyclopedia of Telecommunications*. John Wiley and Sons, Aug. 2003, ch. Concatenated convolutional codes and iterative decoding.

[10] M. Tüchler, A. Singer, and R. Koetter, "Minimum mean squared error equalization using a priori information," *Signal Processing, IEEE Transactions on*, vol. 50, pp. 673–683, Mar. 2002.

[11] M. Tüchler, R. Koetter, and A. Singer, "Turbo equalization: Principles and new results," *IEEE Transactions on Communications*, vol. 50, pp. 754–767, May 2002.